

# Position-Based ANN Impedance Control for A Three-Fingered Robot Hand

R.L.A. Shauri\*, M.A.A.M. Sabri, A.B. Roslan

School of Electrical Engineering, College of Engineering,  
Universiti Teknologi MARA, 40450 Shah Alam, Selangor, MALAYSIA  
\*ruhizan@uitm.edu.my

## ABSTRACT

A feedforward ANN was previously developed for recognition of two objects i.e. a spongy ball and a plastic bottle but was verified through simulation only. In this work, the feasibility of the ANN model is tested by applying it to the robot's impedance control which takes the exerted force at the finger as input while resulting in an output for the selection rule of the impedance stiffness parameter, named  $K_d$ . From the results, the different object textures can be distinguished by the ANN where the absolute peak values of measured rate force during contact with the ball reached 0.15 N and a slightly higher value of 0.32 N for the bottle.  $K_d$  values were found to switch between 1000 and 250 based on the ANN outputs for the ball and bottle, respectively, thus affecting the dynamics of the fingertip through modified position reference of the fingertip. However, it is also observed that the object was incorrectly classified in some moments when the exerted force was not sufficient due to the weak grasp of the object. This shows that the nonlinear factor from the hardware defects needs to be considered when refining the  $K_d$  selection rule in future studies.

**Keywords:** Artificial Neural Network; Object Recognition; Impedance Control

## Introduction

Human-like robotic hands are a subject of study in robotics that is gaining a lot of attention from the scientific community because of the potential benefits they can provide for object manipulation. The robot hand is typically designed for fluid human-like gestures that are influenced by the human musculoskeletal

system. Due to its intricate structure, building a model and applying a controller to it is one of the challenges in developing a robot hand. Various robotic hands or end effectors that mimic human hand capabilities have been actively explored for applications such as rehabilitation, electronic equipment assembly, servicing, and others that require work that can be done with a fingered hand instead of a typical gripper or suction type.

The ability of robot hands to grasp objects with different textures is an improvement of its feature for object manipulation. When an end effector interacts with an object, the control system needs intelligent force control to make the robot hand modify the fingers' position accordingly.

As one of the methods for pattern recognition, Artificial Neural Network (ANN) has been a good choice with great potential for various control system applications. A neural network is an interconnected assembly of simple processing elements, units, or nodes, that operate like human neurons. The input layer, output layer, hidden layer, neuron/node, weight, bias, activation function, and learning function make up the basic structure of an ANN. The processing ability of the network is stored in the inter-unit connection strengths, or weights, obtained by a process of adaptation to or learning from a set of training patterns. This means that during the learning process, the output will be compared with the targets to update the knowledge of the network stored in the weight of the nodes. This repeats iteratively until the ANN response to each pattern is close to the corresponding target [1]. The organization and selection of the basic structure to suit the control requirement for a system distinguishes each form of ANN. Every type of ANN is different based on the arrangement and selection of the basic structure to suit the requirement of the control system. Examples of ANN techniques for approximating nonlinear functions include Recurrent Neural Networks (RNN), Convolution Neural Networks (CNN), and Radial Basis Functions (RBF) which are widely used by many studies in various engineering and non-engineering fields.

The application of ANN for real robot control has been researched by several studies. Sun *et al.* [2] for instance, have developed a novel observer using the ANN inverse method to provide the speed information of a bearingless induction motor to the control loop of the system. The effectiveness of the observer in providing the speed estimation was proven by experimental results, thus reducing the cost for speed measurement using ANN and its applicability for good performance and stability of the motor speed control.

Meanwhile, a study by Al-Gallaf *et al.* [3] proposed a method to calculate grasping and manipulation forces using ANN. The contact forces between the hand joint space torques and the consequent object forces were calculated using a quadratic optimization method before being learned by ANN. The work proved the ability of ANN in providing the relationship between the fingertip forces and joint torques including faster computation

times compared to the conventional Jacobian calculation. ANN was also being applied to predict tool life used in milling operations such as in the work by [4]. Three parameters that are usually used to analyse the milling process consisting of cutting speed, feed rate, and depth of cut were used to train the ANN. The predicted model and experimental results achieved a good correlation of about 0.97 and 0.95 on the training and test data, respectively, thus showing that the three parameters are significant to be used for the tool life prediction. A similar study was implemented by [5] to model an ANN as the observer to estimate force for the force control of a robot end-effector. Due to the very strong nonlinear friction effects from the pulley and cable used to move the robot end-effector, the force data of the cable tension is hard to measure accurately. Thus, ANN which was trained with the force data measured by force sensors located at each winch of the motors was used to feed the measured data back to the force control. The results from the experiment showed the applicability of ANN to provide the force estimation for compensating the friction for the robot control. Work by [6] also focused on controlling a 3-fingered robot gripper based on feedback force data measured by a modified force sensitive resistor (FSR) sensor. They analysed the response from finger position, motor current, and force data for grasping low and high stiffness of objects. The work however has not applied any intelligent method to use the measured force data for the force control of the gripper.

ANN has also been applied in a study that used muscle signals to control the motion of a five-fingered robot hand [7]. In this work, the authors proposed a feature recognition method using ANN on the collected muscle data to produce 16 hand motions output to move the robot hand. Real-time hand gestures made by a wearable MYO gesture armband were successfully recognized with an accuracy of 89.38%. Borja and Lescano [8] have proposed an ANN method to generate the trajectory of a robotic arm based on camera images of the end effector position. No sensor was needed to measure the joint position of the arm except for the two cameras placed on the robot. Each six main movements in forward, backward, right, left, up, and down directions was produced by the supervised learning ANN consisting of six perceptrons for each direction of the robot DOF to bring the end effector to the corrected position. The experimental test showed an acceptable absolute error of 0.43 cm, but the calculation of the end effector position can be significantly affected by the changing environment and light exposure of the scene which is a disadvantage when using camera images as ANN data for learning.

Deep learning ANN was used to predict the walking gaits of a user who wears an assistive robot mechanism for the lower-limb part [9]. The CNN was developed to learn kinematic and muscle activity signals data collected from electrogoniometer (GONIO), surface electromyography (EMG), and internal measurement unit (IMU) sensors worn by users when doing locomotor activities. As a result, CNN was observed to be able to predict the user intent

for walking with a classification of 1.11%. Apart from using ANN for generating trajectories based on sensors or for solving control variables, a study by [10] used feedforward ANN to derive a complicated robot kinematics model consisting of not only the 3D position but also the roll-pitch-yaw orientation of the robot. The ANN architecture was trained to incorporate differential relationships in the model for forward kinematics and trigonometric equations for orientation. Then, the kinematic ANN model was validated in simulation tests on a 7-DoF robot and a soft robot to make an infinity-shaped path. This is followed by real experiments with a 7-DoF KUKA IIWA LBR arm robot to make square and infinity-shaped paths. The position and orientation of the path tracking errors in the simulation test for the proposed method were slightly improved compared to the ANN structure without the incorporation of the differential relationships. Meanwhile, the real experiments with the proposed ANN resulted in about 16 mm to 44 mm position errors and considerably small orientation errors for both paths used.

Another recent research work involving a neural network method for a 6-DoF KUKA LBR IIWA robot with a bio-inspired soft gripper (FESTO DHEF-20-A) was proposed by [11] where they have developed a deep learning algorithm to help the soft gripper pick novel objects. The first version of their end-to-end neural network called BIG-Net I was presented in [12] and improved further in this work with a revised name BIG-Net II. The ANN was trained with a massive dataset of pixel-wise grasp parameters which consist of grasp poses, grasp quality, and gripping steps. The depth images of each grasp scene were captured by a camera mounted on the robot's wrist during the object grasping experiments by the robot. The estimated grasp direction, quality, and gripping steps for the chameleon-tongue-inspired gripper were observed to provide good grasp feasibility based on the deformation result of the soft gripping pad and gripping forces during the simulation test. The gripper achieved average grasp success rates of more than 90% for household and adversarial objects in real grasping experiments, thus proving the feasibility of their ANN method for the very nonlinear soft robot control.

Interestingly, the same authors came up with another deep learning algorithm called gripping attention convolutional neural network (GA-CNN) for another type of gripper with the same robot [13]. The method focuses on the crucial region of the gripping pad i.e. the deformation and force-torque wrench, to predict the grasp quality by the vacuum gripper. The real-time point cloud data from image processing of the gripping pad and gripper force-torque wrench are integrated into the closed-loop control to detect feasible grasp poses while monitoring the grasp status. The same KUKA LBR IIWA with a different gripper named FORMHAND FH-R150 was used to verify the method with satisfying results which as discussed by the authors were due to the difficulty of estimating the poses of reflective transparent objects and limited resolution of the depth camera for capturing good data.

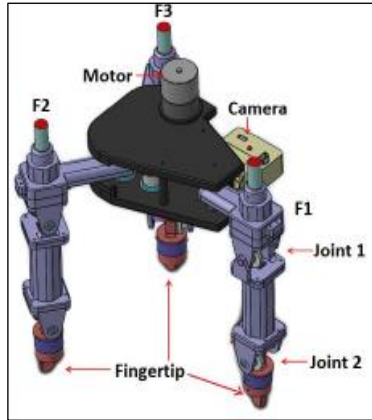
From the above-related studies, it can be observed that ANN has been used in wide applications, especially for systems with nonlinearities. However, besides works by [3], [5], and [11]-[13], there are still a limited number of studies that specifically applied the ANN method for force control of robot hands. Furthermore, these researchers applied different parameters of forces which are measured with different sensors and on different structures of robot hands. Works by [7]-[8] and [9] have also applied ANN but instead of using force data, they have used muscle data or camera data as the ANN inputs for the robot control. On the other hand, even though [6] also investigates robot dynamic responses and measured force when dealing with different object stiffness, the work is limited to the analysis stage only.

The work discussed in this paper is similar to [3], [5], and [11] but the parameters of forces that they have used which include cable tension forces, hand torque data, and gripping forces, respectively, are different from this work which takes the exerted force during object grasping and force rate. Besides, different robot structures such as the cable-driven robot hand and bio-inspired soft gripper robot structure used by these studies require different robot kinematics for the control algorithm compared to the three-fingered robot hand used in this study. In this study, ANN is used for selecting suitable stiffness force parameter values for the fingered robot hand when attending to different object textures, thus producing varied softness or dynamics of the finger. A supervised learning feedforward ANN investigated in a previous study [14] was used with the weight and bias values for each neuron in the network updated using the backpropagation learning technique. In the study, force data collected from a series of object grasping experiments by the robot hand were used in the ANN training and analysed by [15] to attain the relationship between different object textures and impedance stiffness parameters. The validation of the ANN recognition for the object texture and stiffness parameter value however was implemented through simulation only and has not been verified using the actual robot hardware. Therefore, in this study, modifications to the control algorithm have been made to integrate the ANN model into the existing position-based impedance control for generating the finger trajectory. This is followed by verification through real-time experiments with real force measurements provided by a newly installed 6-axis force/torque (F/T) sensor to provide direct input to the ANN.

## **Robot Hand System and Impedance Control**

The 3D hand design and the fabricated three-fingered robot developed in the previous study are shown in Figure 1. The fingered robot hand consists of three fingers with 2-DoF and two links each, joined by a palm as the base of the robot hand [16]. The actuation is provided by DC micro motors while the force exerted on the finger was initially measured by load cells placed inside the

fingertip [17]. Position control and force control were applied in the inner control loop and the outer control loop, respectively, using Matlab Simulink and Real-time Workshop [18]-[19]. However, due to the inconsistency of the movable part of the fingertip to press the load cell sensors placed beneath the fingertip structure, an improved fingertip design was later applied which embeds 6-axis force-torque (F/T) sensors (Figure 1(c)) to replace the load cells.



(a)



(b)

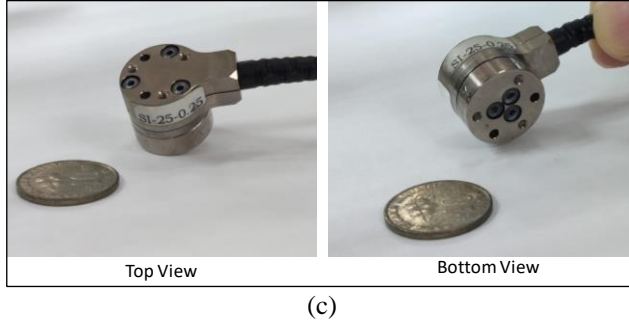


Figure 1: (a) 3D mechanical hand design [16], (b) the fabricated three-fingered robot hand, and (c) the new F/T sensor installed in the finger

The interface between the hardware and software using multiple PCI boards namely PCI NI 6225 and PCI Advantech was introduced by [20] to obtain both encoders and force sensor measurements. The system architecture shown in Figure 2 illustrates the connection between the sensors, actuators, and controllers of the complete system. The measured force signal is sent to the analog input block of Simulink through PCI NI 6225 while the digital input block in Simulink receives pulse signals from channels A and B of the encoders through PCI Advantech 1771. Concurrently, the actuation signal from PID control is passed to the motor driver through the PCI Advantech 1771.

The two-control loop system block diagram is shown in Figure 3. The translational impedance equation is used to develop the position-based impedance control, which ensures an adequate mass-spring-dashpot characteristic for the position displacement when the end-effector makes contact with the environment [19]. When the fingers grasp an object, external forces  $f_{ext}$  provided by the sensor will give the measure of how strong the force is being exerted on the finger. If the impedance control system is activated when  $f_{ext}$  exceeds a threshold force  $f_{ref}$ , the required change of position will be calculated to modify the desired tip-end location  $P_d$  to its new position  $P_{d\_new}$ . Applying the optimal value of impedance parameters i.e. the impedance mass  $M_d$ , impedance damping  $D_d$ , and impedance stiffness  $K_d$  that have been selected from an observation experimental work by [21], different softness of the robot finger can be produced based on the feedback force measurement.

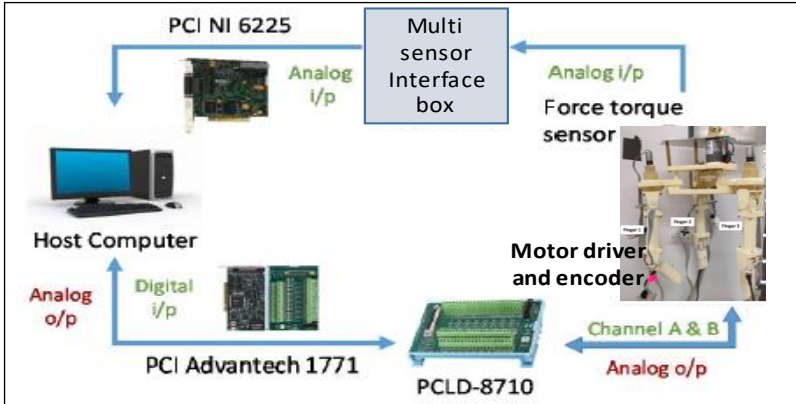


Figure 2: The interface architecture using multiple PCIs

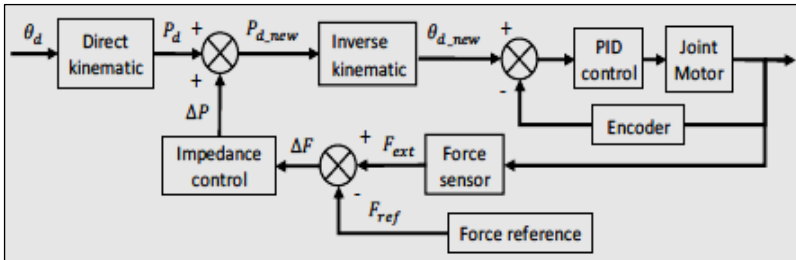


Figure 3: The position-based impedance control

## ANN-Based Force Control

Applying an intelligent algorithm for force control is to identify the uncertainties in the hand system and to reduce the effect of state constraints through the learning process [22].

### Modification of impedance control method

In robot control, uncertainties in the robot control such as friction between bearings, gears, and linkages, and forces exerted on the finger by the different hardness of objects require a method that could learn and adjust the control parameter accordingly. Upon determination of the impedance stiffness parameter for different hardness of grasped objects, unlike [6] that used finger position, motor current, and force measurements for their force control, this study has used two force parameters which are the measured exerted force and force rate learned by ANN. Conversely, different approaches introduced by



[11] and [12] have used ANN on learned image data instead to control their soft gripper picks object.

In this study, in order to extend the flexibility of the control that has been previously introduced by [19] and [21], the selection of impedance parameter  $K_d$  needs to be done automatically by the system based on real-time measured values. Therefore, a feedforward ANN has been studied by [14] where the performance between three different training methods was compared via Matlab simulation to verify ANN's capability in recognizing two object textures based on force data collected during several grasping experiments. The ANN model from the best training method was added to the control system block diagram as shown in Figure 4 to improve the existing control system. Conceptually, the ANN model from the study was expected to produce the output signals that will be used to select suitable  $K_d$  values for the impedance block but unfortunately the verification of the work has not been done. It is important that the capability of the ANN method to change  $K_d$  values according to the texture of the object i.e. in this case a harder plastic bottle or softer spongy ball, can be confirmed. Therefore, in this study, the ANN model was integrated with the existing position-based impedance control algorithm in Simulink programming and tested on the robot hardware in real-time. The output range from ANN recognition based on the real-time force measurements was observed to write the  $K_d$  selection rule algorithm before providing it to the impedance control block.

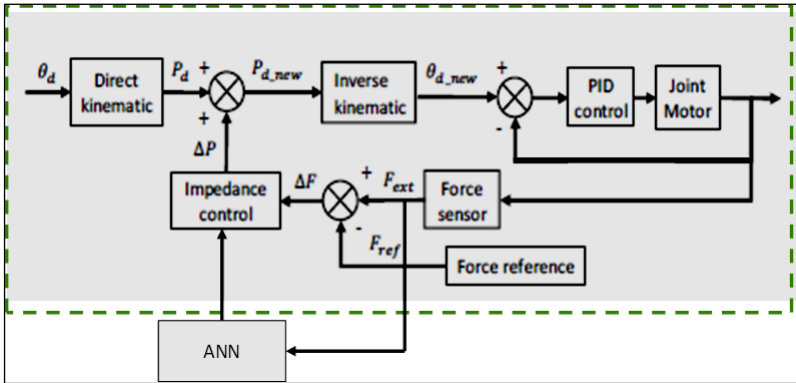


Figure 4: Position-based impedance control with feedforward ANN

The above ANN block consists of the subsystem shown in Figure 5. As outlined in the blue dotted line, the ANN model trained by [14] labelled as a pattern recognition neural network block receives two inputs called  $f_{rate}$  and  $f_{ext}$  from the force sensor and produces output that carries two values with the

labels ANN\_1 and ANN\_2. The number of the ANN output was decided based on the ANN structure that has been designed in previous work.

$f_{rate}$  is the difference between the initial external force  $f_{ext,i}$  and the final external force  $f_{ext,f}$  divided by the time taken for the robot finger to grasp the object.  $f_{ext,i}$  is the force exerted on the robot finger when grasping the object after 0.25 seconds while the  $f_{ext,f}$  is the force exerted on the finger when grasping the object after 1 second, which is a slightly delayed time to confirm the grasp. Consequently, both ANN\_1 and ANN\_2 outputs were used as the input variable in the Embedded MATLAB function 1 (green outlined block) to determine the object texture which is between the spongy ball or the plastic bottle and as a reference to select  $K_d$  value. The  $K_d$  selection rule will be discussed in the next subsection using graph results from the simulation test.

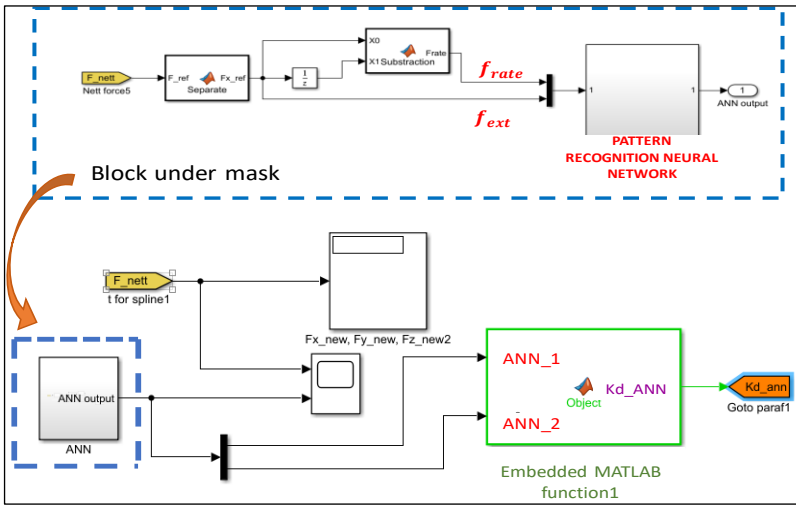


Figure 5: Subsystem ANN block

### Selection of $K_d$ by object texture

In order to design the rule for  $K_d$  related to the ANN outputs, the previous simulation results from [14] need to be analysed. The comparison between  $f_{rate}$  values for different  $K_d$  between ball and bottle grasping has been discussed by [14] where  $K_d$  for the bottle is observed to be good at 250 while  $K_d$  for the ball is 1000. The implications of changing the  $K_d$  value will enable the robot's fingertips to grasp objects of different textures with sufficient force.

### Creating rule for $K_d$ selection based on ANN outputs

A simulation test was implemented to verify the position-based ANN impedance control using real force data as input by directly pressing the robot

fingertip by hand. Figure 6 shows the comparison graph between the net force in the x-axis direction  $f_{nett_x}$  with the ANN outputs.  $f_{nett_x}$  is defined in (1) as the net force of  $f_{ext}$  by subtracting the  $f_{ext}$  when contact starts with the  $f_{ext}$  before the contact, where the initial value is set to 0. Here, the net force  $f_{nett_x}$  is taken as input to the ANN instead of the raw  $f_{ext}$  because  $f_{ext}$  includes not only the exerted force from the grasping that is needed but also the force applied by the cover of the fingertip onto the embedded sensor.

The blue, grey, and orange lines indicate  $f_{nett_x}$ , ANN\_2 and ANN\_1, respectively. It can be observed that output ANN\_1 becomes higher than output ANN\_2 when  $f_{nett_x}$  is exceeds a threshold value of about 1.1 N. Conversely, output ANN\_2 becomes higher than output ANN\_1 when  $f_{nett_x}$  is lower than the threshold value. Thus, it can be concluded that when higher force is exerted on the robot fingertip, higher  $f_{nett_x}$  will result in higher output ANN\_1. Otherwise, lower  $f_{nett_x}$  will result in higher ANN\_2. This shows that the ANN algorithm is able to produce significant output ANN\_1 and ANN\_2 according to the different  $f_{nett_x}$  values.

$$f_{nett_x} = \text{contact } f_{nett_x} - \text{before contact } f_{nett_x}, \text{ where } f_{nett_x}(0) = 0 \quad (1)$$

Furthermore, as observed from the same graph, 0.5 can be taken as the threshold value of the ANN output when both ANN\_1 and ANN\_2 are opposite to each other. Hence, combining this observation with the  $K_d$  value for ball and bottle discussed in the previous section, the condition for selecting  $K_d$  based on ANN outputs can be written as in Equation (2).

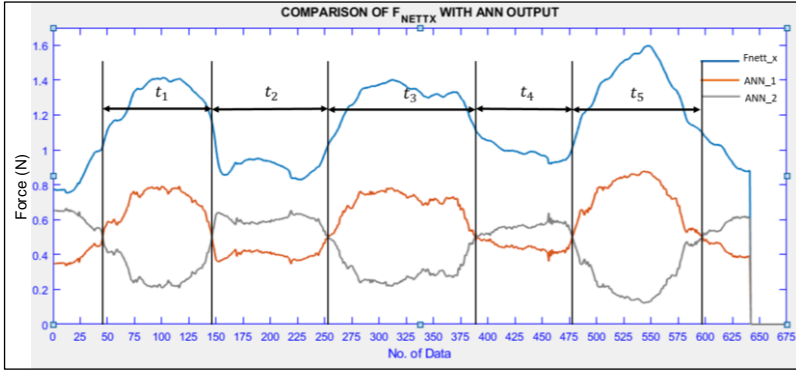


Figure 6: Comparison of simulation data  $f_{nett_x}$  with ANN outputs

$$K_d = \begin{cases} 1000 & , \quad ANN_1 < 0.5 \text{ AND } ANN_2 > 0.5 \\ 250 & , \quad ANN_1 > 0.5 \text{ AND } ANN_2 < 0.5 \\ 500 & , \quad \text{Otherwise} \end{cases} \quad (2)$$

### Grasping experiment

The desired fingertip position was calculated using forward kinematic equations of the finger derived by [19] based on the desired joint angles set by the user. When the robot finger moves to the desired position to grasp the object, the measurement of  $f_{ext}$  and the encoder were taken in real-time as feedback signals for the two-loop control of the ANN force control system. Only  $f_{ext}$  in the x-axis direction measured from finger 1 was used since all fingers were set to produce synchronous inward movement to the centre of the palm for the grasping motion. For observation and analysis, ANN output and force data during the grasping test were collected and discussed. Besides, the modified reference position  $P_{d\_new}$  and reference  $P_d$  or  $P_{d\_ref}$  (as can be seen from the block diagram in Figure 4) were also graphed and compared to observe the modification of position by the proposed algorithm according to the measured  $f_{ext}$ . Here, the position reference will be modified when  $f_{ext}$  exceeds the threshold force reference,  $f_{ref}$ . Figure 7 depicts the experimental setup in which the chosen objects were the same objects used for the ANN object texture recognition trained by [14]. A flowchart as shown in Figure 8 explains the flow of parameter calculation by the ANN and the control algorithm to produce the changes to the finger position based on the force measured during the grasping.

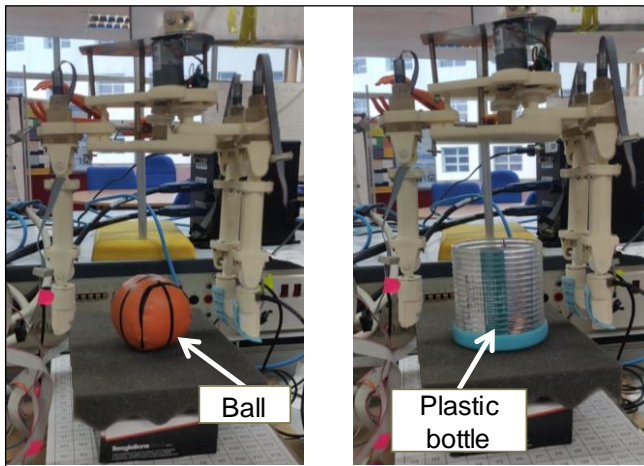


Figure 7: Experiment setup for grasping task of a spongy ball (left) and a plastic bottle (right)

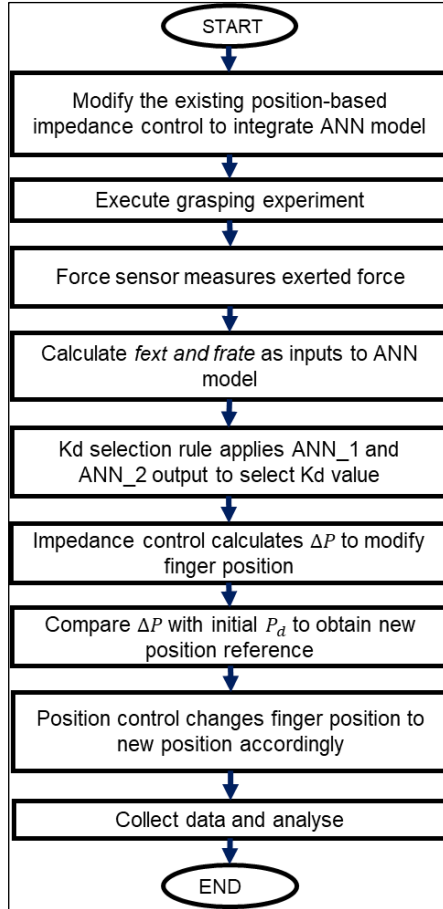


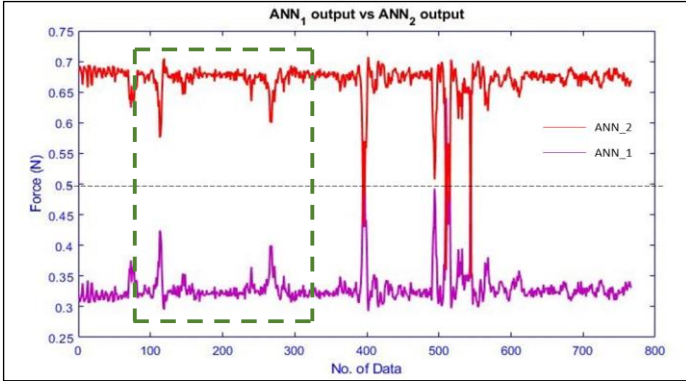
Figure 8: Flowchart of parameter calculation

## Results and Discussion

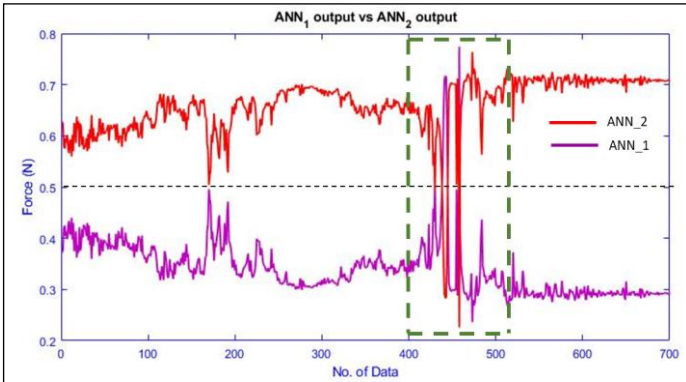
### Comparison between ANN outputs when grasping ball and bottle

Data from the grasping experiments were collected every 1 ms sampling time to observe the outputs from the ANN model developed by [14] and the applicability of  $K_d$  selection rule created in Equation (2). Graphs in Figure 9 show ANN\_1 and ANN\_2 outputs indicated by the purple and red lines, respectively. It can be shown from Figure 9(a) that ANN\_2 value consistently stays higher than ANN\_1 most of the time during the grasping state of the ball. On the other hand, Figure 9(b) shows that the ANN\_1 output starts to increase

while ANN\_2 decreases at the same time for the bottle case. In Figure 9(b), at one point when the grip on the bottle was strong enough, ANN\_1 oppositely exceeds ANN\_2 as highlighted by the green dashed line. Therefore, it can be concluded that when the ANN\_1 is lower than 0.5 and ANN\_2 is higher than 0.5, the grasped object can be recognized as a ball. Conversely, if the ANN\_1 is higher than 0.5 while the ANN\_2 is lower than 0.5, the object can be recognized as a bottle. Thus, these results complied with the condition rule written in Equation (2).



(a)



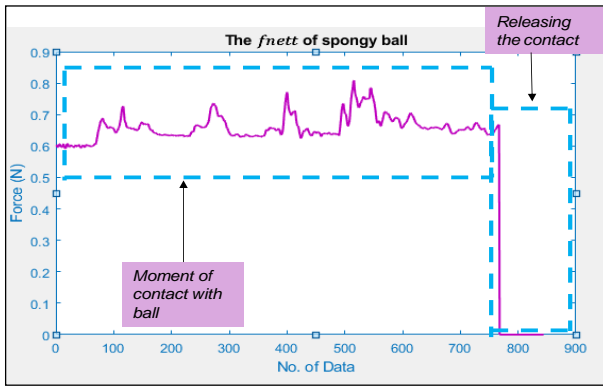
(b)

Figure 9: Comparing ANN outputs; (a) when grasping a ball, and (b) when grasping a bottle

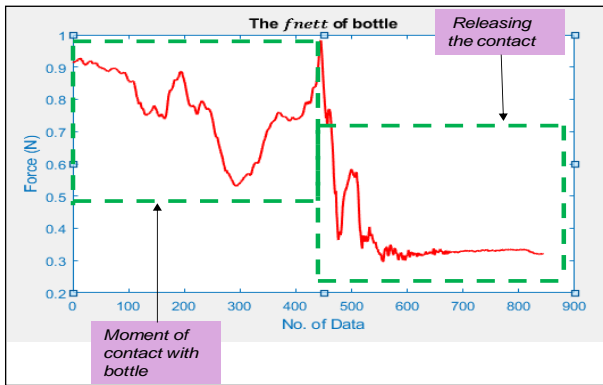
### Grasping experiment results for $f_{nett}$ and modified position $P_{d\_new}$

Figures 10(a) and 10(b) show the measured  $f_{nett}$  when the robot grasped both objects, respectively. Moving from the standby position, the fingertip received

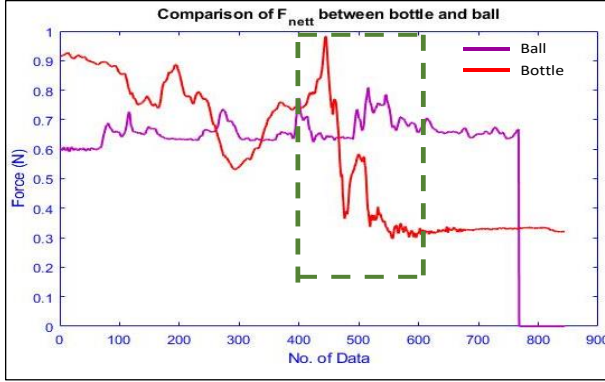
an increasing external force when it started making contact with the object. As the fingertips moved toward the desired position while pressing the object,  $f_{nett}$  increased significantly and dropped instantly once it released the grasp, as can be shown in both figures for the ball and bottle. The average of  $f_{nett}$  ball during the contact is between 0.65 N to 0.75 N. On the other hand, the average of  $f_{nett}$  bottle during the contact is higher which is between 0.8 N to 0.9 N. This concludes that the  $f_{nett}$  bottle is higher than the  $f_{nett}$  ball as can be seen clearly in the comparison graphs in Figure 10(c), which also agrees with the observation made by [15] regarding the force data analysis from the grasping of the same objects. The finger released the grasp at about after 750th data for ball grasping, and at about after 650th data for the bottle.



(a)



(b)



(c)

Figure 10:  $f_{nett}$  measurement during and after grasping; (a) for ball, (b) for bottle, and (c) for both overlapped on one graph

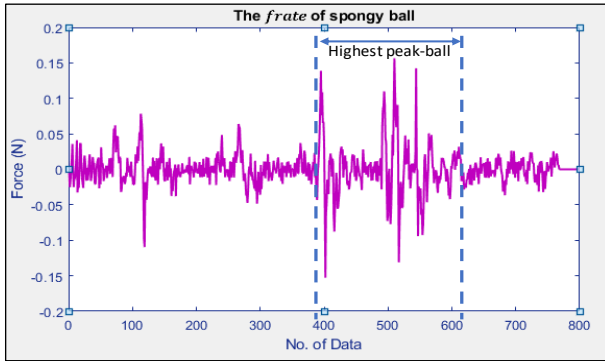
Next,  $f_{rate}$  and modified position reference when the finger made contact with the objects will be discussed. It can be observed from Figure 11 (a) that the absolute peak values of  $f_{rate}$  during contact with the ball reached 0.15 N between 400th to 600th data while from Figure 11(b) during contact with the bottle, the absolute peak value reached 0.32 N between 450th to 650th data. This proves that the measurement of force could provide the feel of touch to the robot finger to distinguish the soft and hard textures of objects during grasping.

Consequently, Figures 11(c) and 11(d) depict the modified reference position during the ball and bottle grasping experiments, respectively. Figure 11(c) shows that the proposed control was able to calculate the new robot's tip-end position  $P_{d\_new}$  from its initial set position at 0.07943 m in the z-axis as depicted by the reference  $P_d$  or  $P_{d\_ref}$  in the orange line. Similarly, Figure 11(d) shows that the proposed control has modified  $P_{d\_new}$  from  $P_{d\_ref}$  that was initially set at 0.08448 m in the z-axis, as depicted in the orange line. Highest change in the position can be seen between the 400th to 600th data and 400th to 650th data, respectively, which matches with the duration of peak measured forces for both objects. It can be concluded that different intensities of force received by the robot finger could modify the dynamic and the fingertip position thus making the finger flexible for grasping different objects.

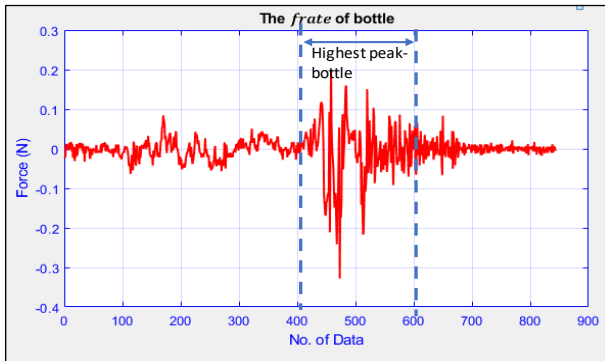
Figures 12(a) and 12(b) show the  $K_d$  values that have been selected automatically by the method based on the ANN outputs during the grasping experiments.  $K_d$  has been selected at 1000 since there was no contact between the robot's finger and the object at the beginning, which is correct and follows the rules written in Equation (2). In fact, this can be ignored because this value does not give effect to any object since no grasping has happened yet.



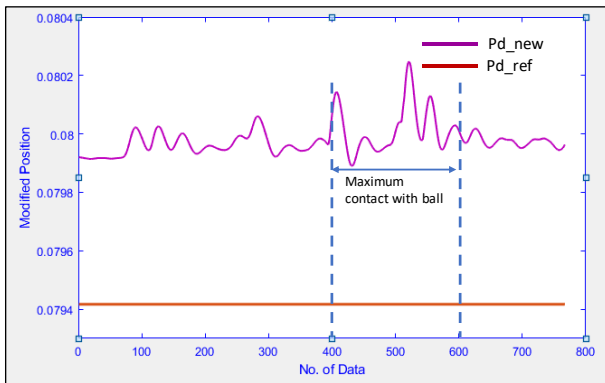
According to the rule,  $K_d$  for the ball should be selected at 1000, and 250 for the bottle case.



(a)



(b)



(c)

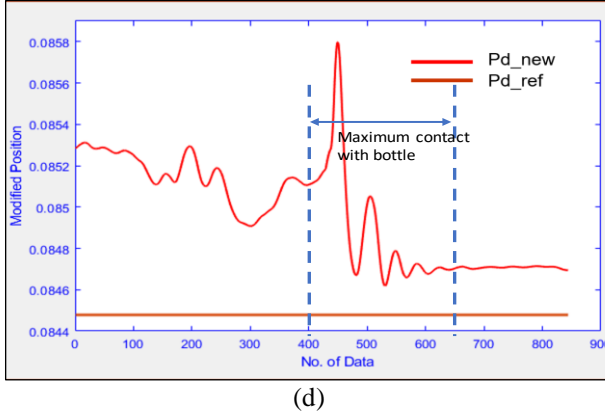
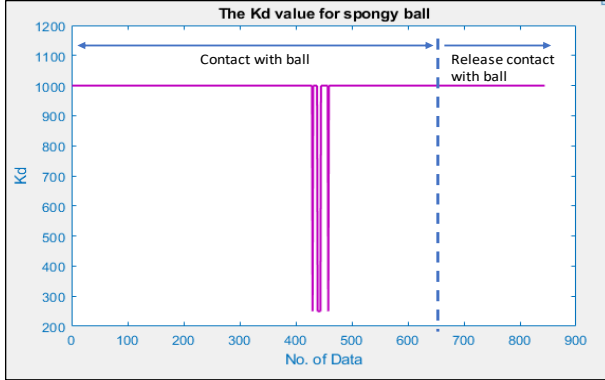


Figure 11: (a)  $f_{rate}$  of ball, (b)  $f_{rate}$  of bottle, (c) modified reference position – ball, and (d) modified reference position – bottle

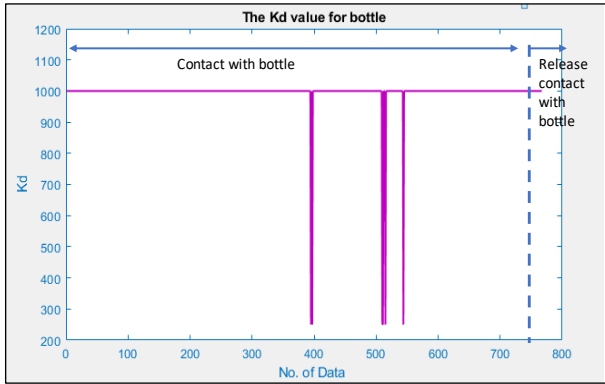
When contact with the ball happened,  $K_d$  has been calculated correctly to remain at 1000 except between 420th and 450th data. These short intervals where  $K_d$  changed to 250 was due to the loose gear or fingers' connection at the joints that have caused weakened grasping force by the fingers at times. On the other hand, for bottle case, there have been few moments when  $K_d$  has been correctly selected at 250 and as discussed earlier in Figure 10(b) and Figure 10(d), these were the moments when the maximum contact with the bottle happened.

The above results prove that the ANN could produce different  $K_d$  to the impedance control when the finger grasps the bottle or the ball. However, this also reveals some moments where the algorithm faced difficulty in classifying the object based on the ANN outputs against the 0.5 threshold as in Equation (2) when the exerted force is not sufficient due to the weak grasp of the object by the hand. Therefore, more data collection for in-depth analysis is required to improve the parameter selection rule for  $K_d$  in the future considering the effect of worn-out hardware on the force measurement.

Producing softness of the finger by adjusting the desired position when receiving a certain force level was proven by [19] for the same robot hand. The control algorithm however selected the impedance parameter based on observation and intuitive decisions from experiment data for attending only one object. Comparatively, the application of ANN to autonomously decide the impedance parameter in this paper is new to the robot hand and has shown improvement in the position-based impedance control of the robot system when attending to two different hardness of objects.



(a)



(b)

Figure 12: Automatically selected  $K_d$  by ANN. (a)  $K_d$  for ball, and (b)  $K_d$  for bottle

## Conclusion

A position-based ANN impedance control was executed on a three-fingered robot hand based on exerted force measured by the F/T sensor during object grasping. The ANN model which was trained in a separate study was used to recognize two types of object textures i.e. a spongy ball and a plastic bottle, based on real force data collected from a series of grasping experiments. To operate the control algorithm, the measured force signals were given as the input to the ANN model while the output was used to select the value of the impedance stiffness parameter  $K_d$  for providing different softness of the finger when grasping objects with different textures. From the grasping test, it can be

observed that the soft and hard object textures can be distinguished by the method where the absolute peak value of the measured rate force during contact with the ball reached 0.15 N and a slightly higher value of 0.32 N for the bottle. Furthermore, the result on the generated position reference showed that the proposed control was able to modify the robot's tip-end position from its initial position according to the amount of exerted force and selected  $K_d$  based on the ANN outputs.  $K_d$  values were found to switch between 1000 and 250 for ball and bottle, respectively according to the output from ANN when sufficient force was measured and this complies with the  $K_d$  selection rule. However, the objects were incorrectly classified in some moments when the exerted force was not sufficient due to the weak grasp of the object by the hand. Therefore, more data collection for in-depth analysis is required to improve the parameter selection rule for  $K_d$  in the future study. The current results however give meaningful sight in realizing the idea and proof of concept for the application of ANN-based impedance control for a very non-linear robot hand system using real-time measured force data.

## **Contributions of Authors**

The authors confirm the equal contribution in each part of this work. All authors reviewed and approved the final version of this work.

## **Funding**

This research is fully supported by the Ministry of Higher Education (MOHE) (FRGS/1/2019/TK04/UITM/02/9) grant. The authors acknowledged the Ministry of Higher Education (MoHE) for the approved fund and to Universiti Teknologi MARA for providing the laboratory space and equipment.

## **Conflict of Interests**

All authors declare that they have no conflicts of interest.

## **Acknowledgment**

The authors would like to thank the Ministry of Higher Education (MOHE) for providing the financial support for this research. The authors also thank the School of Electrical Engineering, College of Engineering, Universiti

Teknologi MARA (UiTM) Shah Alam for providing the facilities and the equipment.

## References

- [1] K. Gurney, *An Introduction to Neural Networks*, 1st ed. London: Taylor & Francis, Inc., 1997.
- [2] X. Sun, L. Chen, Z. Yang and H. Zhu, "Speed-sensorless vector control of a bearingless induction motor with artificial neural network inverse speed observer", *IEEE/ASME Transactions on Mechatronics*, vol. 18, no. 4, pp. 1357-1366, 2013.
- [3] E. Al-Gallaf, K. Al Mutib and H. Hamdan, "Artificial neural network dexterous robotics hand optimal control methodology: Grasping and manipulation forces optimization", *Artificial Life and Robotics*, vol. 15, no. 4, pp. 408-412, 2010.
- [4] A. M. Khorasani, M. Reza Soleymani Yazdi and M. S. Safizadeh, "Tool life prediction in face milling machining of 7075 al by using artificial neural networks (ANN) and Taguchi design of experiment (DOE)," *International Journal of Engineering and Technology*, vol. 3, no. 1, pp. 30-35, 2011.
- [5] J. Piao, E. -S. Kim, H. Choi, H. C. -B. Moon, E. Choi, J. -O. Park, C. -S. Kim, "Indirect force control of a cable-driven parallel robot: Tension estimation using artificial neural network trained by force sensor measurements", *Sensor*, vol. 19, no. 11, p. 2520, 2019.
- [6] A. S. Sadun, J. Jalani and F. Jamil, "Grasping analysis for a 3-finger adaptive robot gripper," 2016 2nd IEEE International Symposium on Robotics and Manufacturing Automation (ROMA), Ipoh, Malaysia, pp. 1-6, 2016.
- [7] G. -C. Luh, Y. -H. Ma, C. -J. Yen and H. -A. Lin, "Muscle-gesture robot hand control based on sEMG signals with wavelet transform features and neural network classifier," *2016 International Conference on Machine Learning and Cybernetics (ICMLC), Jeju, Korea (South)*, pp. 627-632, 2016.
- [8] M. G. Borja Borja and S. Lescano, "New heuristic method merging artificial vision and neural networks used in a sensorless robotic arm position control," in *Proceeding 2020 IEEE ANDESCON*, pp. 1-6, 2020.
- [9] U. H. Lee, J. Bi, R. Patel, D. Fouhey and E. Rouse, "Image transformation and CNNs: a strategy for encoding human locomotor intent for autonomous wearable robots", *IEEE Robotics and Automation Letters*, vol. 5, no. 4, pp. 5440-5447, 2020.
- [10] F. Cursi, W. Bai, W. Li, E. M. Yeatman and P. Kormushev, "Augmented neural network for full robot kinematic modelling in SE(3)", *IEEE Robotics and Automation Letters*, vol. 7, no. 3, pp. 7140-7147, 2022.

- [11] H. Zhang, Y. Wu, E. Demeester and K. Kellens, "BIG-Net: Deep learning for grasping with a bio-inspired soft gripper," *IEEE Robotics and Automation Letters*, vol. 8, no. 2, pp. 584-591, Feb. 2023.
- [12] H. Zhang, J. Peeters, E. Demeester, and K. Kellens, "A CNN-based grasp planning method for random picking of unknown objects with a vacuum gripper," *Journal of Intelligent & Robot Systems*, vol. 103, no. 64, pp. 1-19, 2021.
- [13] H. Zhang, J. Peeters, E. Demeester and K. Kellens, "Deep learning reactive robotic grasping with a versatile vacuum gripper", *IEEE Transactions on Robotics*, vol. 39, no. 2, pp. 1244-1259, 2023.
- [14] A. B. Roslan and R. L. A. Shauri, "Object Texture Recognition Based on Grasping Force Data Using Feedforward Neural Network," *Journal of Electrical & Electronic Systems Research*, vol. 20, pp. 77-83, 2022.
- [15] M. S. Selamat, "The effect of impedance control stiffness to the grasping force for different object textures," M.S. Thesis, School of Electrical Engineering, Universiti Teknologi MARA, Shah Alam, Malaysia, 2021.
- [16] J. Jaafar and R. L. A. Shauri, "Three-fingered robot hand for assembly works," in *Proceeding of 2013 IEEE 3rd International Conference on System Engineering and Technology*, pp. 237-241, 2013.
- [17] J. Jaafar and R. L. A. Shauri, "Fingertip structural analysis simulated design evaluation," *Jurnal Teknologi*, vol. 76, no. 4, pp. 25-29, 2015.
- [18] M. K. M. Kasim, R. L. A. Shauri and K. Nasir, "PID position control of three-fingered hand for different grasping styles," in *Proceeding of 2015 6th IEEE Control and System Graduate Research Colloquium*, pp. 7-10, 2016.
- [19] K. Nasir, R. L. A. Shauri, N. M. Salleh and N. H. Remeli, "Kinematic modelling for PID position control of a new three-fingered robotic hand," *ARPN Journal of Engineering and Applied Sciences*, vol. 14, no.2, pp. 335-343, 2019.
- [20] R. L. A. Shauri, A. B. Roslan and Z. S. M. Zarib, "Application of 6-axis force torque (F/T) sensor for a three fingered robot hand impedance control," in *Proceeding of 2020 IEEE 10th International Conference on System Engineering and Technology*, pp. 262-266, 2020.
- [21] K. Nasir, R. L. A. Shauri, N. M. Salleh and N. H. Remeli, "Effects of varying impedance parameters for position-based impedance control of a three-fingered robot hand," *Pertanika Journal of Science and Technology*, vol. 25, pp. 111-122, 2017.
- [22] A. B. Roslan and R. L. A. Shauri, "Non-intelligent and intelligent force control for robotic applications: a review," *ASM Science Journal*, vol.16, pp. 1-13, 2021.